Joint International Topical Meeting on Mathematics & Computation and Supercomputing in Nuclear Applications (M&C + SNA 2007)
Monterey, California, April 15-19, 2007, on CD-ROM, American Nuclear Society, LaGrange Park, IL (2007)

A FOKKER-PLANCK METHOD FOR MODELING COMPTON SCATTERING IN IMPLICIT MONTE CARLO SIMULATIONS

Jeffery D. Densmore and James S. Warsa
Computational Physics and Methods Group, Los Alamos National Laboratory
P.O. Box 1663, MS D409, Los Alamos, NM 87545, USA
jdd@lanl.gov; warsa@lanl.gov

Jim E. Morel
Department of Nuclear Engineering, Texas A&M University
3133 TAMU, College Station, TX 77843, USA
morel@tamu.edu

ABSTRACT

We present a new method for modeling Compton scattering in Implicit Monte Carlo (IMC) simulations that implicitly evaluates the radiation-matter energy coupling due to photon-electron scattering. In this technique, the scattering physics are split from the radiative-transfer process and represented by a Fokker-Planck approximation. In each time step, radiative transfer, minus Compton scattering, is simulated using the usual IMC method. The results of this calculation are then used to solve the Fokker-Planck equation deterministically and update the material temperature and radiation intensity accordingly. With a set of numerical examples, we demonstrate that our new Fokker-Planck method is able to employ larger time steps than an analog technique for simulating Compton scattering that evaluates the material temperature explicitly.

Key Words: Radiative transfer; Implicit Monte Carlo; Compton scattering; Fokker-Planck approximation; Kompaneets' equation

1. INTRODUCTION

The Implicit Monte Carlo (IMC) method [1] is an effective technique for solving nonlinear, time-dependent radiative-transfer problems via Monte Carlo simulation. In IMC, the energy coupling of radiation and matter through the absorption and emission of photons is semi-implicitly approximated by an effective-scatter process. This effective scattering helps stabilize the calculation, allowing the use of larger time steps than a purely explicit method (where radiation energy absorbed in a given time step cannot be re-emitted until the following time step) [2–4].

In addition to absorption and emission, the scattering of photons by free electrons also provides an energy coupling between radiation and matter [5]. In this process, known as Compton scattering, the frequency change of a scattered photon results in an energy transfer between the photon and the target electron. Canfield, Howard, and Liang have developed an analog Monte Carlo method for simulating the photon-electron scattering kinematics that has the capacity to be very accurate [6]. However, when this technique is employed in a time-dependent problem, the temperature describing the electron velocity distribution is explicitly evaluated. The analog method does not update this temperature until the end of the time step, a situation that results in a conditionally stable calculation.

In this paper, we present a new technique for modeling Compton scattering in IMC simulations that implicitly evaluates the energy coupling due to photon-electron scattering. In our new method, the scattering physics are split from the radiative-transfer process and represented by a Fokker-Planck approximation [7–10]. The resulting time and frequency-dependent partial-differential equation, also known as *Kompaneets' equation*, models changes in photon frequency and the corresponding energy coupling due to Compton scattering, but neglects any angular changes. This approximation is valid when the photon frequency and material temperature are small with respect to the electron rest mass, conditions that exist in many problems of interest. In each time step, we first simulate radiative transfer, minus Compton scattering, by employing the usual IMC method. Next, we use the results of the IMC calculation as an initial condition for the Fokker-Planck equation and implicitly solve this equation with existing deterministic techniques [11]. The solution to the Fokker-Planck equation then serves as an initial condition for the IMC simulation in the following time step. Similar splitting methods have been developed for modeling Compton scattering in deterministic radiative-transfer calculations [12, 13]. In this paper, we specifically adapt these techniques for use with IMC. Although our new method is an approximate representation of Compton scattering, we expect this scheme can employ larger time steps than the analog technique because the energy coupling is implicitly evaluated.

In the remainder of this paper, we briefly review the equations governing nonlinear, time-dependent radiative transfer, the corresponding IMC method, and the analog technique for simulating Compton scattering. We then develop our Fokker-Planck method and show how it can be combined with standard IMC. Next, we use a set of numerical examples to demonstrate that our new Fokker-Planck technique can employ larger time steps than the analog method without suffering from instabilities. We conclude with a brief discussion.

2. RADIATIVE TRANSFER AND IMPLICIT MONTE CARLO

The equations governing nonlinear, time-dependent radiative transfer are [5]

$$\frac{1}{c}\frac{\partial I}{\partial t} + \mathbf{\Omega}\cdot\boldsymbol{\nabla} I + (\sigma_a + \sigma_s)I = \int\int \frac{\nu}{\nu'}\sigma_s(\mathbf{r}, \nu' \rightarrow \nu, \mathbf{\Omega}'\cdot\mathbf{\Omega}, T)I(\mathbf{r}, \mathbf{\Omega}', \nu', t)d\nu' d\mathbf{\Omega}' + \sigma_a B \quad , \tag{1}$$

and

$$C_v\frac{\partial T}{\partial t} = \int\int \sigma_a(I - B)d\nu d\mathbf{\Omega} + \int\int\int\int \left(1 - \frac{\nu}{\nu'}\right)\sigma_s(\mathbf{r}, \nu' \rightarrow \nu, \mathbf{\Omega}'\cdot\mathbf{\Omega}, T)I(\mathbf{r}, \mathbf{\Omega}', \nu', t)d\nu' d\mathbf{\Omega}' d\nu d\mathbf{\Omega} \quad . \tag{2}$$

Here, $\mathbf{r}$ is the spatial variable, $\mathbf{\Omega}$ is the angular variable, ν is the frequency variable, t is the temporal variable, $I(\mathbf{r}, \mathbf{\Omega}, \nu, t)$ is the radiation intensity, $T(\mathbf{r}, t)$ is the material temperature, $\sigma_a(\mathbf{r}, \nu, T)$ is the absorption opacity, $\sigma_s(\mathbf{r}, \nu, T)$ is the total scattering opacity, $C_v(\mathbf{r}, T)$ is the heat capacity, and c is the speed of light. In addition, the Planck function is defined by

$$B(\nu, T) = \frac{2h\nu^3}{c^2}\frac{1}{e^{h\nu/kT} - 1} \quad , \tag{3}$$

where h is Planck's constant and k is Boltzmann's constant. Also, the total and differential scattering opacities are related by

$$\sigma_s(\mathbf{r}, \nu, T) = \int\int \sigma_s(\mathbf{r}, \nu \rightarrow \nu', \mathbf{\Omega}\cdot\mathbf{\Omega}', T)d\nu' d\mathbf{\Omega}' \quad . \tag{4}$$

Note that we have neglected induced scattering in Eqs. (1) and (2), a physical effect that would make the scattering terms nonlinear functions of the radiation intensity. The analog method that will be discussed in Section 3 does not model induced scattering. Thus, we will not consider induced scattering in this paper in order to provide a fair comparison between the analog technique and our new Fokker-Planck method, a scheme that can be extended to include induced scattering. We will consider this improvement in future work.

To solve Eqs. (1) and (2) using IMC, we first prescribe a temporal grid $0 = t_0 < t_1 < t_2 < \cdots$. Then, within each time step $t_n < t < t_{n+1}$, the emission source on the right side of Eq. (1) is semi-implicitly approximated using Eq. (2). The resulting IMC equations are [1]

$$\frac{1}{c}\frac{\partial I}{\partial t} + \mathbf{\Omega}\cdot\mathbf{\nabla} I + (\sigma_{a,n} + \sigma_s)I = \int\int \frac{\nu}{\nu'}\sigma_s(\mathbf{r}, \nu' \rightarrow \nu, \mathbf{\Omega}'\cdot\mathbf{\Omega}, T)I(\mathbf{r}, \mathbf{\Omega}', \nu', t)d\nu' d\mathbf{\Omega}' + \frac{1}{4\pi}\frac{\sigma_{a,n}b_n}{\sigma_{p,n}}\int\int(1-f_n)\sigma_{a,n}(\mathbf{r},\nu')I(\mathbf{r},\mathbf{\Omega}',\nu',t)d\nu' d\mathbf{\Omega}' + \frac{1}{4\pi}\frac{\sigma_{a,n}b_n}{\sigma_{p,n}}f_n\sigma_{p,n}acT_n^4 \quad , \quad (5)$$

and

$$C_v\frac{\partial T}{\partial t} = \int\int f_n\sigma_{a,n}I d\nu d\mathbf{\Omega} - f_n\sigma_{p,n}acT_n^4 + \int\int\int\int\left(1-\frac{\nu}{\nu'}\right)\sigma_s(\mathbf{r},\nu'\rightarrow\nu,\mathbf{\Omega}'\cdot\mathbf{\Omega},T)I(\mathbf{r},\mathbf{\Omega}',\nu',t)d\nu' d\mathbf{\Omega}' d\nu d\mathbf{\Omega} \quad , \quad (6)$$

where the subscript n refers to quantities evaluated at their beginning-of-time-step values. In Eqs. (5) and (6), we have defined the *Fleck factor* f_n as

$$f_n = \frac{1}{1+\beta_n c\sigma_{p,n}\Delta t_n} \quad , \quad (7)$$

where

$$\beta_n = \frac{4aT_n^3}{C_{v,n}} \quad , \quad (8)$$

and $\Delta t = t_{n+1} - t_n$ is the size of the time step. In addition, the Planck-averaged absorption opacity is given by

$$\sigma_{p,n}(\mathbf{r}) = \int \sigma_{a,n}(\mathbf{r},\nu)b_n(\nu)d\nu \quad , \quad (9)$$

where $b(\nu, T)$ is the normalized Planck function such that

$$B(\nu, T) = \frac{1}{4\pi}acT^4 b(\nu, T) \quad , \quad (10)$$

and a is the radiation constant.

Note that in Eqs. (5) and (6) we have represented a fraction f_n of the physical absorption opacity as an effective absorption opacity and a fraction $1 - f_n$ as an effective scattering opacity. Accordingly, we have reduced the emission source by a factor f_n. Also, we have not included any temporal approximations to the Compton-scattering terms. In the following sections, we will discuss two techniques for modeling Compton scattering in IMC simulations.

3. AN ANALOG COMPTON-SCATTERING METHOD

In the analog method, the total scattering opacity is first evaluated at the beginning-of-time-step material temperature. Then, Eqs. (5) and (6) can be simulated in a manner similar to the usual IMC technique. When a particle undergoes a Compton scatter, the new frequency and direction are determined using a procedure due to Canfield, Howard, and Liang [6]. This sampling technique is summarized as follows:

1. sample a target electron velocity from a relativistic Maxwellian distribution at the explicit value of the material temperature
2. Lorentz transform the particle frequency and direction from the laboratory frame to the electron rest frame
3. process the scattering kinematics in the electron rest frame
4. Lorentz transform the new particle frequency and direction from the electron rest frame back to the laboratory frame
5. account for radiation-matter energy transfer using the frequency change in the laboratory frame

Compton scattering in the electron rest frame is governed by the Klein-Nishina model, and thus existing techniques can be employed to sample the new frequency and direction in Step 3 [14, 15]. We note that this procedure is equivalent to explicitly evaluating the material temperature in the Compton-scattering terms in Eqs. (5) and (6). The analog method has the capacity to be very accurate, as the scattering kinematics are modeled exactly. However, as we will see, the explicit evaluation of the material temperature leads to a conditionally stable algorithm.

4. A FOKKER-PLANCK COMPTON-SCATTERING METHOD

We now present a new method for simulating Compton scattering that is based on a Fokker-Planck approximation. In this technique, we split the scattering physics from the remainder of the radiative-transfer process. Then, from Eqs. (5) and (6), the resulting IMC equations are

$$\frac{1}{c}\frac{\partial I}{\partial t} + \mathbf{\Omega}\cdot\mathbf{\nabla} I + \sigma_{a,n} I = \frac{1}{4\pi}\frac{\sigma_{a,n} b_n}{\sigma_{p,n}} \int\int (1-f_n)\sigma_{a,n}(\mathbf{r},\nu') I(\mathbf{r},\mathbf{\Omega}',\nu',t) d\nu' d\mathbf{\Omega}' + \frac{1}{4\pi}\frac{\sigma_{a,n} b_n}{\sigma_{p,n}} f_n \sigma_{p,n} a c T_n^4 \quad , \quad (11)$$

and

$$C_v \frac{\partial T}{\partial t} = \int\int f_n \sigma_{a,n} I d\nu d\mathbf{\Omega} - f_n \sigma_{p,n} a c T_n^4 \quad . \quad (12)$$

Similarly, the equations corresponding to Compton scattering are

$$\frac{1}{c}\frac{\partial I}{\partial t} + \sigma_s I = \int\int \frac{\nu}{\nu'}\sigma_s(\mathbf{r},\nu'\rightarrow\nu,\mathbf{\Omega}'\cdot\mathbf{\Omega},T) I(\mathbf{r},\mathbf{\Omega}',\nu',t) d\nu' d\mathbf{\Omega}' \quad , \quad (13)$$

and

$$C_v \frac{\partial T}{\partial t} = \int\int\int\int \left(1-\frac{\nu}{\nu'}\right)\sigma_s(\mathbf{r},\nu'\rightarrow\nu,\mathbf{\Omega}'\cdot\mathbf{\Omega},T) I(\mathbf{r},\mathbf{\Omega}',\nu',t) d\nu' d\mathbf{\Omega}' d\nu d\mathbf{\Omega} \quad . \quad (14)$$

The Fokker-Planck approximation to Eq. (13) replaces the integral scattering operator with a frequency-dependent differential operator by assuming that the photon frequency and material temperature are small with respect to the electron rest mass, i.e.,

$$\frac{h\nu}{mc^2} \ll 1 \quad \text{and} \quad \frac{kT}{mc^2} \ll 1 \quad , \tag{15}$$

where mc^2 is the electron rest mass in energy units. The resulting Kompaneets' equation is [7–10]

$$\frac{1}{\sigma_{\text{Th}}c}\frac{\partial E}{\partial t} = \nu\frac{\partial}{\partial \nu}\left[\nu\frac{kT}{mc^2}\frac{\partial E}{\partial \nu} + \left(\frac{h\nu}{mc^2} - 3\frac{kT}{mc^2}\right)E\right] \quad . \tag{16}$$

Here, we have defined the spectral radiation energy density as

$$E(\mathbf{r},\nu,t) = \frac{1}{c}\int I(\mathbf{r},\mathbf{\Omega},\nu,t)d\mathbf{\Omega} \quad . \tag{17}$$

In addition, $\sigma_{\text{Th}}(\mathbf{r})$ is the Thomson opacity, a quantity that is independent of photon frequency and material temperature and proportional to the electron density. Equation (16) is slightly different than the usual form of Kompaneets' equation, since we have neglected induced scattering. Using this standard Kompaneets' equation would allow the addition of induced scattering to our methodology. We also replace Eq. (14) with

$$C_v\frac{\partial T}{\partial t} = -\int \frac{\partial E}{\partial t}d\nu \quad , \tag{18}$$

an equation for the material temperature that imposes energy conservation. The derivation of Eq. (16) employs an angularly averaged radiation intensity. Thus, our replacement of the integral scattering operator in Eq. (13) with the Fokker-Planck approximation neglects the angular effects of Compton scattering.

To solve Eq. (16), we first specify a multigroup frequency structure $\nu_{1/2} < \nu_{3/2} < \cdots < \nu_{G+1/2}$ consisting of G frequency groups. Typically, IMC simulations already employ such a group structure for representing the absorption and total scattering opacities. Next, using an implicit temporal discretization and a frequency discretization due to Larsen, *et al.* [11] allows us to rewrite Eq. (16) as

$$\frac{E_{n+1,g} - E_{n+1/2,g}}{\sigma_{\text{Th}}c\Delta t_n} = \frac{\nu_g}{\Delta\nu_g}\left(S_{g+1/2} - S_{g-1/2}\right) \quad , \quad 1 \le g \le G \quad , \tag{19}$$

where

$$S_{g+1/2} = \begin{cases} 0 \quad , & g = 0 \text{ or } g = G \quad , \\ \dfrac{h\nu_{g+1/2}^4}{mc^2}\dfrac{\nu_{g+1}^{-3}e^{h\nu_{g+1}/kT_{n+1}}E_{n+1,g+1} - \nu_g^{-3}e^{h\nu_g/kT_{n+1}}E_{n+1,g}}{e^{h\nu_{g+1}/kT_{n+1}} - e^{h\nu_g/kT_{n+1}}} \quad , & 1 \le g \le G-1 \quad . \end{cases} \tag{20}$$

Here, the subscript g refers to quantities evaluated at frequency-group centers, and $\Delta\nu_g = \nu_{g+1/2} - \nu_{g-1/2}$ is the frequency-group width. The subscript $n + 1/2$ denotes intermediate values of the operator split, i.e., the solution to Eqs. (11) and (12) that serves as the initial condition for Eqs. (16)–(18). Note that Eqs. (19)–(20) form a tridiagonal linear system of G equations for fixed T_{n+1}. In a manner analogous to the way Eq. (16) was discretized, we approximate Eq. (18) as

$$C_v\left(T_{n+1} - T_{n+1/2}\right) = -\sum_{g=1}^{G}\left(E_{n+1,g} - E_{n+1/2,g}\right)\Delta\nu_g \quad . \tag{21}$$

This equation assumes a temperature-independent heat capacity, although our methodology can easily be extended to a more complicated equation of state.

Equations (19) and (21) represent a nonlinear system of $G+1$ equations for the end-of-time step material temperature and spectral radiation energy density. We reduce this system to a single nonlinear equation for T_{n+1} by eliminating $E_{n+1,g}$ from Eq. (21) using Eq. (19). We then solve the resulting equation using the Brent-Dekker method, a bracketing technique, from the GNU Scientific Library [16]. Each function evaluation requires a nested, tridiagonal matrix inversion, a process that is quite efficient. After T_{n+1} is determined, we can solve Eq. (19) a final time to calculate $E_{n+1,g}$. We note that Eqs. (19) and (21) must be solved by nonlinear iteration to ensure the radiation-matter energy coupling due to Compton scattering is implicitly evaluated.

Our new Fokker-Planck method now proceeds as follows. First, we simulate Eq. (11) with a standard IMC calculation. With the results of this simulation, we determine $T_{n+1/2}$ using Eq. (12) and employ the census particles (i.e., particles that reach the end of the time step) to estimate $E_{n+1/2,g}$ using Eq. (17). Equations (19) and (21) are then solved as described above to calculate T_{n+1} and $E_{n+1,g}$. The end-of-time-step spectral radiation energy density allows us to represent the end-of-time-step radiation intensity as

$$I_{n+1}(\mathbf{r},\mathbf{\Omega},\nu) = c\left[\sum_{g=1}^{G} E_{n+1,g}(\mathbf{r})\Delta\nu_g\right]\left[\frac{E_{n+1,g}(\mathbf{r})}{\sum_{g=1}^{G} E_{n+1,g}(\mathbf{r})\Delta\nu_g}\right]\left[\frac{\int I_{n+1/2}(\mathbf{r},\mathbf{\Omega},\nu)d\nu}{\int\int I_{n+1/2}(\mathbf{r},\mathbf{\Omega},\nu)d\nu d\mathbf{\Omega}}\right] \quad , \quad (22)$$

for $\nu_{g-1/2} < \nu < \nu_{g+1/2}$. The final step in our Fokker-Planck method is to modify the properties of the census particles so that they represent this intensity. The first bracketed term in Eq. (22) is the total radiation energy density (i.e., the spectral radiation energy density integrated over all frequencies). In order to rigorously conserve energy, the energy weights of the census particles are adjusted as follows:

$$\text{ew}_{\text{new}} = \left(\frac{\sum_{g=1}^{G} E_{n+1,g}\Delta\nu_g}{\sum_{g=1}^{G} E_{n+1/2,g}\Delta\nu_g}\right)\text{ew}_{\text{old}} \quad . \quad (23)$$

Here, ew_{new} and ew_{old} are the new and old energy weights, respectively, of a given census particle. The second bracketed term in Eq. (22) represents the radiation frequency distribution. This term can be viewed as a histogram probability distribution function that is constant in each group and can be sampled to determine the new frequency of a census particle. The last term in Eq. (22) is the radiation angular distribution. This distribution is unchanged by the Fokker-Planck solution, and thus we leave the directions of census particles unmodified.

Note that the Fokker-Planck approximation treats the spatial variable $\mathbf{r}$ as a parameter. In practice, IMC calculations employ a spatial grid with the material temperature (and temperature-dependent quantities) represented as a piecewise-constant function. Thus, our Fokker-Planck method can be independently employed in each spatial cell to update the material temperature and adjust census particles in that cell.

5. NUMERICAL RESULTS

We now compare our new Fokker-Planck technique for modeling Compton scattering in IMC simulations to the analog method with an infinite-medium test problem. This problem consists of a purely scattering material (i.e., $\sigma_a = 0$) with an initial material temperature of $kT = 10.0$ keV and an initial radiation intensity defined by a Planck function at a temperature of $kT = 1.0$ keV. The Thomson opacity is $\sigma_{\text{Th}} = 1.0$ cm^{-1} and the heat capacity is temperature independent with a value of $C_v = 0.01$ jk/cm^3/keV (1 jerk = 1 jk = 10^9 joules). Since the radiation is initially "cooler" than the material, photons will gain energy at the expense of the material until the material temperature decreases to an equilibrium value.

We simulated this problem with both Compton-scattering methods using a variety of time-step sizes. Each calculation employed 1 million particles per time step and a frequency-group structure with $0.0 \text{ keV} < h\nu < 100.0$ keV and 100 linearly spaced groups. For the analog method, a temperature and frequency-dependent fit was used to calculate the total scattering opacity from the Thomson opacity [17].

The material temperature generated using a time-step size of $\Delta t = 0.1$ sh (1 shake = 1 sh = 10^{-8} seconds) is plotted in Fig. 1. Here, and in subsequent figures, the analog and Fokker-Planck methods are compared to a benchmark solution generated with the analog technique and $\Delta t = 0.001$ sh. We note that both methods reproduce the initial transient, although with some truncation error. The Fokker-Planck equilibrium solution is slightly low due to the frequency discretization employed in Eq. (19). This error could be reduced by using more frequency groups or a logarithmically spaced group structure. In addition, the Fokker-Planck calculation was approximately 80 times faster than the analog simulation. This increase in efficiency is due to the replacement of many Monte Carlo scattering events over a time step with the deterministic solution of a nonlinear equation at the end of the time step.

As the time-step size is increased, the performance of the analog method begins to deteriorate. The analog-method material temperature using $\Delta t = 0.2$ sh is given in Fig. 2. Here, we see that the analog solution oscillates nonphysically about the equilibrium value. Larger time steps produced negative material temperatures, a situation that caused the simulation to stop.

In contrast, the Fokker-Planck method can employ much larger time steps than the analog technique. This behavior is illustrated in Fig. 3. Although the material temperature becomes less accurate over the initial transient with increasing time-step size, the Fokker-Planck method avoids nonphysical oscillations and negative temperatures and yields correct equilibrium solutions.

6. CONCLUSIONS

We have presented a new method for modeling Compton scattering in IMC simulations based on the Fokker-Planck approximation that implicitly evaluates the radiation-mattering energy coupling due to photon-electron scattering. In each time step, we first simulate radiative transfer, minus Compton scattering, employing the usual IMC technique. Next, with the results of this IMC calculation, we deterministically solve the Fokker-Planck equation and update the material temperature and census particles accordingly.

With an infinite-medium test problem, we have demonstrated that our new Fokker-Planck method allows the use of larger time steps than the analog technique, a scheme that evaluates the material temperature explicitly. Specifically, our new method avoids nonphysical oscillations and negative temperatures, a

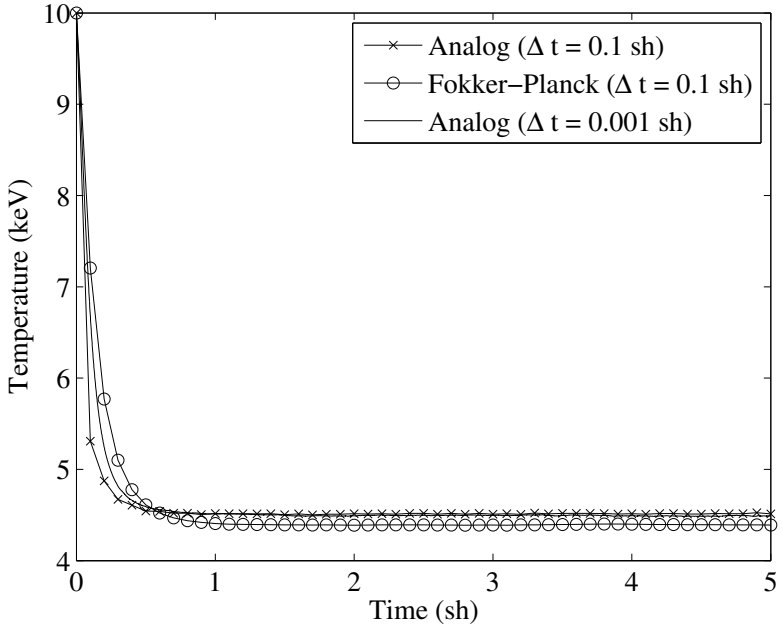

Figure 1. Analog and Fokker-Planck Material Temperature for $\Delta t = 0.1$ sh

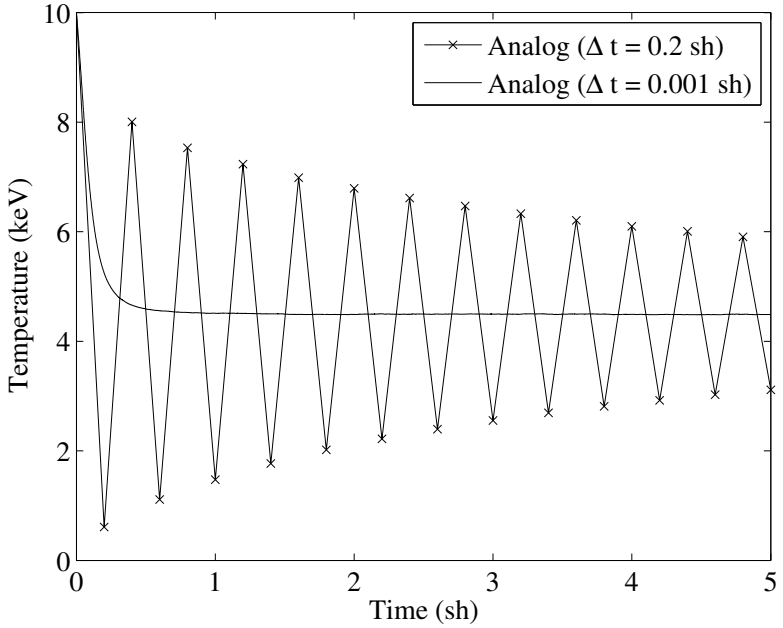

Figure 2. Analog Material Temperature for $\Delta t = 0.2$ sh

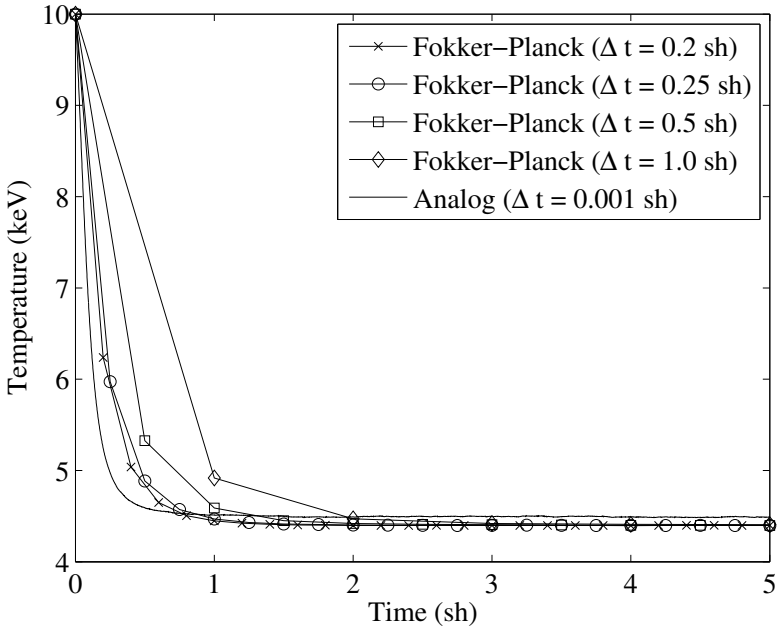

Figure 3. Fokker-Planck Material Temperature for $\Delta t = 0.2$ sh and Larger

situation that causes IMC simulations to stop. In addition, the Fokker-Planck technique is more computationally efficient than the analog scheme since many Monte Carlo scattering events in a given time step are replaced by a deterministic solution of a nonlinear equation at the end of the time step.

Although our Fokker-Planck method accurately models the photon frequency change due to Compton scattering, the angular change is ignored. The directional dependence of scattering, along with the anisotropy of the radiation intensity, is certainly important in practical calculations. The inclusion of angular effects and the testing of our new Fokker-Planck method on space-dependent problems remain for future work.

ACKNOWLEDGMENTS

We would like to thank Aimee Hungerford (Los Alamos National Laboratory) for helpful discussions regarding Compton-scattering physics. This work was performed under U.S. government contract DE-AC52-06NA25396 for Los Alamos National Laboratory, which is operated by Los Alamos National Security, LLC. (LANS) for the U.S. Department of Energy.

REFERENCES

[1] J.A. Fleck, Jr. and J.D. Cummings, "An Implicit Monte Carlo Scheme for Calculating Time and Frequency Dependent Nonlinear Radiation Transport," *J. Comp. Phys.*, **8**, 313 (1971).

[2] E.W. Larsen and B. Mercier, "Analysis of a Monte Carlo Method for Nonlinear Radiative Transfer," *J. Comp. Phys.*, **71**, 50 (1987).

[3] W.R. Martin and F.B. Brown, "Error Modes in Implicit Monte Carlo," *Trans. Amer. Nucl. Soc.*, **85**, 508 (2002).

[4] S.W. Mosher and J.D. Densmore, "Stability and Monotonicity Conditions for Linear, Grey, 0-D Implicit Monte Carlo Calculations," *Trans. Amer. Nucl. Soc.*, **93**, 520 (2005).

[5] G.C. Pomraning, *The Equations of Radiation Hydrodynamics*, Pergamon Press, Oxford, United Kingdom (1973).

[6] E. Canfield, W.M. Howard, and E.P. Liang, "Inverse Comptonization by One-Dimensional Relativistic Electrons," *Astrophys. J.*, **323**, 565 (1987).

[7] A.S. Kompaneets, "The Establishment of Thermal Equilibrium between Quanta and Electrons," *Sov. Phys. JETP*, **4**, 730 (1957).

[8] J.I. Katz, *High Energy Astrophysics*, Addison-Wesley Publishing, Menlo Park, California (1987).

[9] G.B. Rybicki and A.P. Lightman, *Radiative Processes in Astrophysics*, WILEY-VCH, Weinheim, Germany (2004).

[10] J. Castor, *Radiation Hydrodynamics*, Cambridge University Press, Cambridge, United Kingdom (2004).

[11] E.W. Larsen, C.D. Levermore, G.C. Pomraning, and J.G. Sanderson, " Discretization Methods for One-Dimensional Fokker-Planck Operators," *J. Comp. Phys.*, **61**, 359 (1985).

[12] J.E. Morel, "ICS: An Implicit Compton-Fokker-Planck Solver," LA–10855–MS, Los Alamos National Laboratory (1987).

[13] A.M. Winslow, "Multifrequency-Gray Method for Radiation Diffusion with Compton Scattering," *J. Comp. Phys.*, **117**, 262 (1995).

[14] H. Kahn, "Applications of Monte Carlo," AECU–3259, Rand Corporation (1954).

[15] R.N. Blomquist and E.M. Gelbard, "An Assessment of Existing Klein-Nishina Monte Carlo Sampling Methods," *Nucl. Sci. Eng.*, **83**, 380 (1983).

[16] M. Galassi, J. Davies, J. Theiler, B. Gough, G. Jungman, M. Booth, and F. Rossi, *GNU Scientific Library Reference Manual*, Network Theory (2006).

[17] B.R. Wienke, "Relativistic Photon-Maxwellian Electron Cross Sections," *Astron. Astrophys.*, **152**, 336 (1985).